

The Role of Terahertz Polariton Absorption in the Characterization of Crystalline Iron Sulfate Hydrates

Michael T. Ruggiero [†], Tiphaine Bardon[‡], Matija Strlič[‡], Philip F. Taday[§], Timothy M. Korter^{†*}

[†] *Department of Chemistry, Syracuse University, 1-014 Center for Science and Technology, Syracuse, NY 13244-4100, United States*

[‡] *UCL Institute for Sustainable Heritage, Bartlett Faculty of the Built Environment, University College London, 14 Upper Woburn Place, London WC1H 0NN, UK.*

[§] *TeraView Limited, Platinum Building, St John's Innovation Park, Cambridge CB4 0DS, UK.*

*tmkorter@syr.edu

Supplementary Information

List of Figures

Figure S.1. Experimental (black) and calculated (red) PXRD of $\text{FeSO}_4 \cdot 4\text{H}_2\text{O}$.

Figure S.2. Terahertz spectra of $\text{FeSO}_4 \cdot 7\text{H}_2\text{O}$ taken at 225 K (red) and 150 K (blue).

Figure S.3. Experimental PXRD of an $\text{FeSO}_4 \cdot 7\text{H}_2\text{O}$ and $\text{FeSO}_4 \cdot 4\text{H}_2\text{O}$ mixture (black), linear combination of the two individual patterns (red) and the difference (blue).

Figure S.4. Experimental (black) and calculated (red) PXRD of $\text{FeSO}_4 \cdot 7\text{H}_2\text{O}$.

Figure S.5. Experimental (black) and calculated (red) PXRD of $\text{FeSO}_4 \cdot 4\text{H}_2\text{O}$.

Figure S.6. Experimental (black) and calculated (red) PXRD of $\text{Fe}_2(\text{SO}_4)_3\text{OH} \cdot 2\text{H}_2\text{O}$.

Figure S.7. Terahertz spectrum of $\text{FeSO}_4 \cdot \text{H}_2\text{O}$ taken at 77 K.

Figure S.8. Terahertz spectrum of $\text{Fe}_2(\text{SO}_4)_3\text{OH} \cdot 2\text{H}_2\text{O}$ at 77 K.

Figure S.9. 78 K terahertz spectrum of $\text{FeSO}_4 \cdot 4\text{H}_2\text{O}$ with standard deviation in the absorption shown.

List of Tables

Table S.1. Simulated IR-active vibrational frequencies (cm^{-1}) and intensities (km mol^{-1}) of anhydrous FeSO_4 .

Table S.2. Simulated IR-active vibrational frequencies (cm^{-1}) and intensities (km mol^{-1}) of $\text{FeSO}_4 \cdot \text{H}_2\text{O}$.

Table S.3. Simulated IR-active vibrational frequencies (cm^{-1}) and intensities (km mol^{-1}) of $\text{FeSO}_4 \cdot 4\text{H}_2\text{O}$.

Table S.4. Simulated IR-active vibrational frequencies (cm^{-1}) and intensities (km mol^{-1}) of $\text{FeSO}_4 \cdot 7\text{H}_2\text{O}$.

Table S.5. Simulated IR-active vibrational frequencies (cm^{-1}) and intensities (km mol^{-1}) of $\text{Fe}_2(\text{SO}_4)_3\text{OH} \cdot 2\text{H}_2\text{O}$.

Table S.6. Solid-state DFT optimized atomic positions of anhydrous FeSO_4 , which crystallizes $Cmcm$, with lattice parameters $a = 5.251 \text{ \AA}$, $b = 8.020 \text{ \AA}$, $c = 6.642 \text{ \AA}$.

Table S.7. Solid-state DFT optimized atomic positions of $\text{Fe}_2(\text{SO}_4)_3\text{OH} \cdot 2\text{H}_2\text{O}$, which crystallizes $P2_1/m$, with lattice parameters $a = 6.826 \text{ \AA}$, $b = 7.404 \text{ \AA}$, $c = 5.809 \text{ \AA}$, $\beta = 90.254^\circ$.

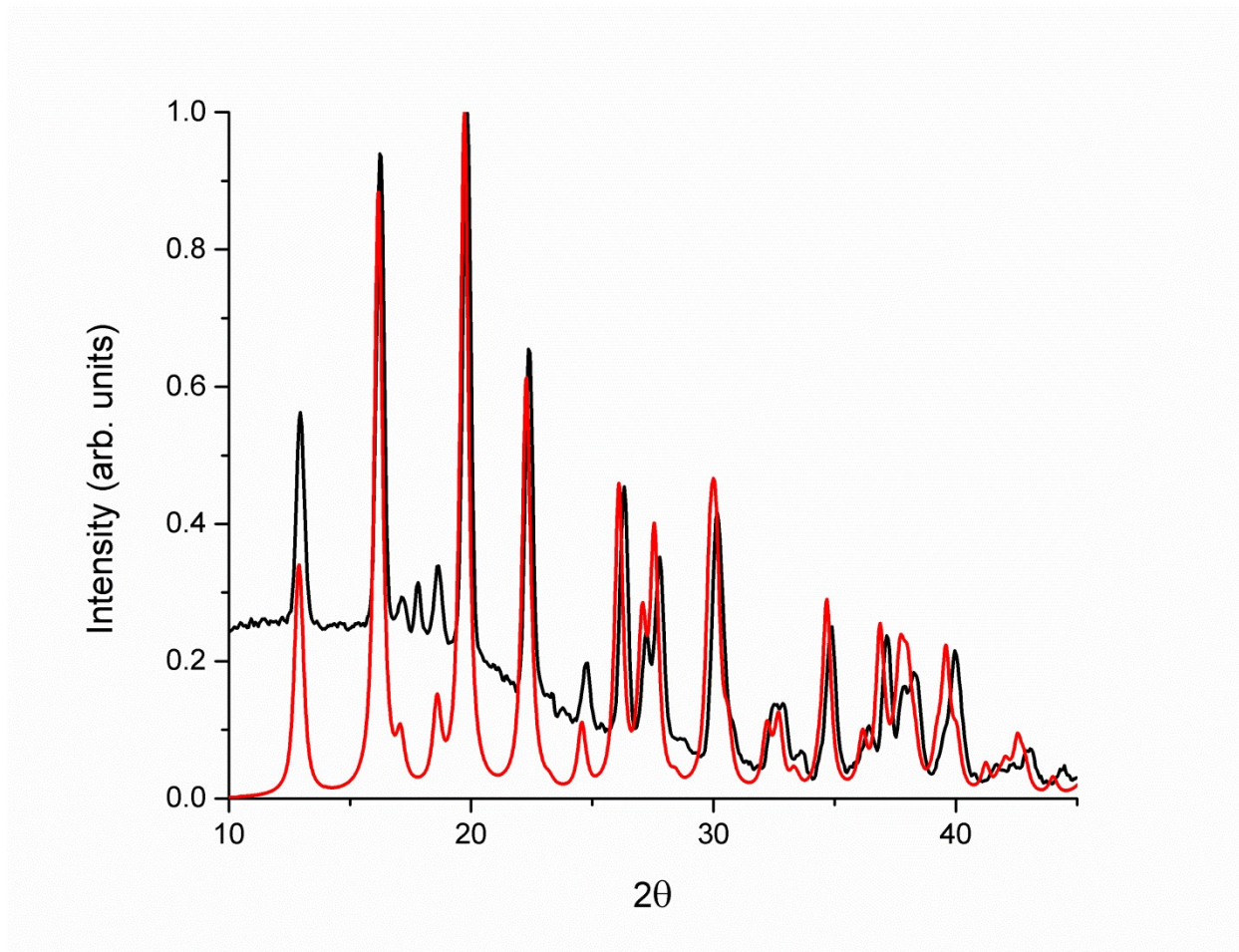


Figure S.1. Experimental (black) and calculated (red) PXR D of FeSO₄ · 4H₂O.

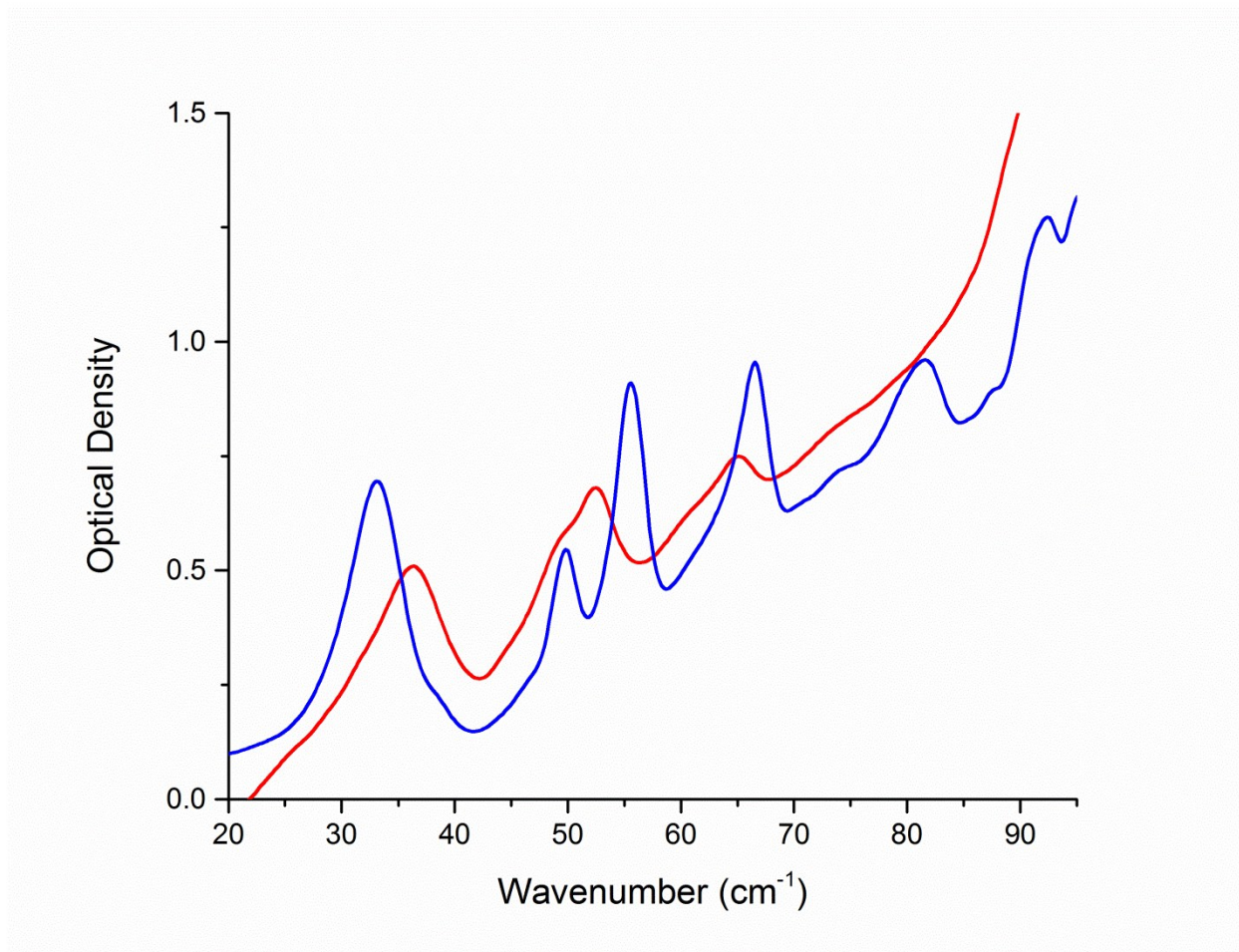


Figure S.2. Terahertz spectra of FeSO₄ · 7H₂O taken at 225 K (red) and 150 K (blue).

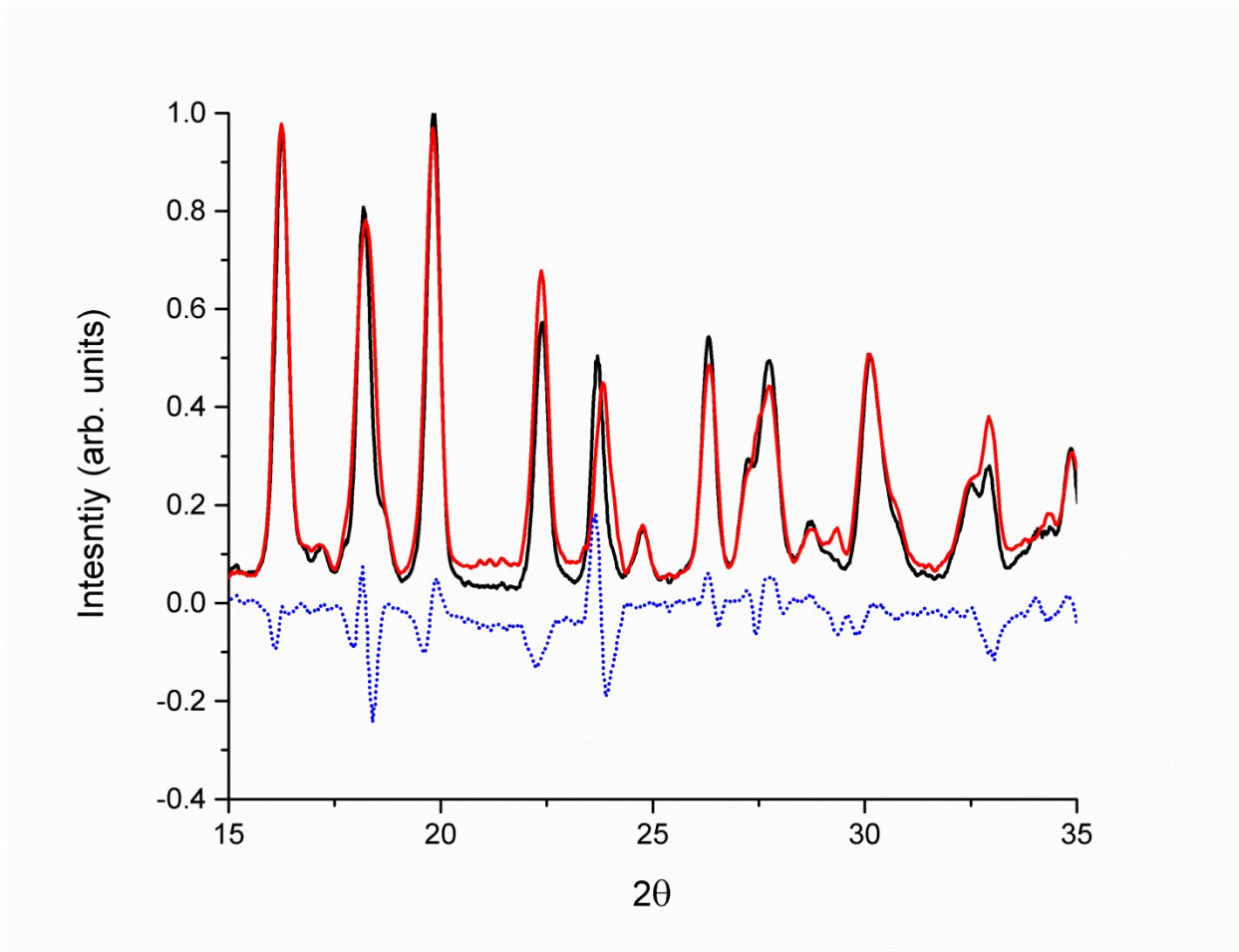


Figure S.3. Experimental PXRD of an $\text{FeSO}_4 \cdot 7\text{H}_2\text{O}$ and $\text{FeSO}_4 \cdot 4\text{H}_2\text{O}$ mixture (black), linear combination of the two individual patterns (red) and the difference (blue).

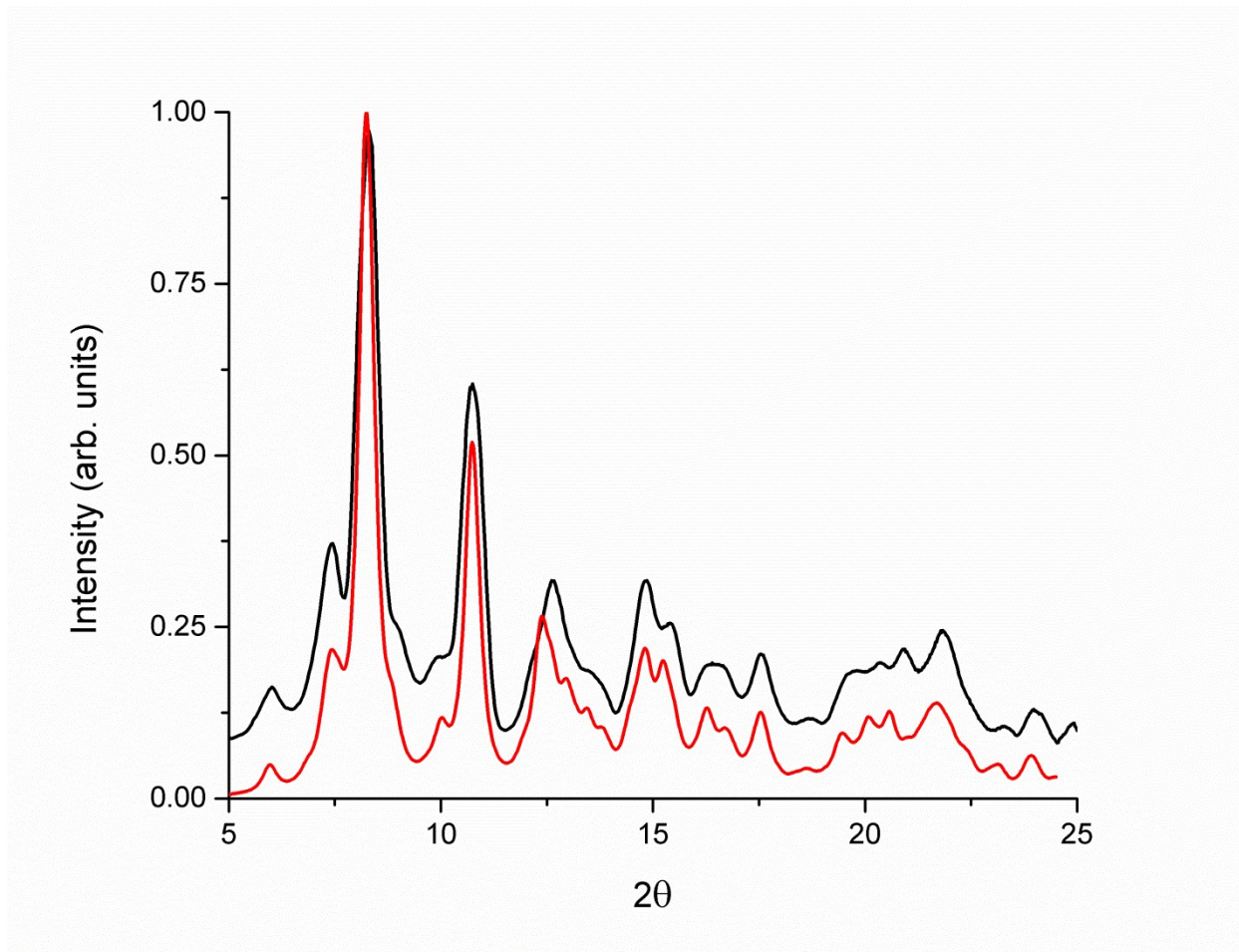


Figure S.4. Experimental (black) and calculated (red) PXR D of FeSO₄ · 7H₂O.

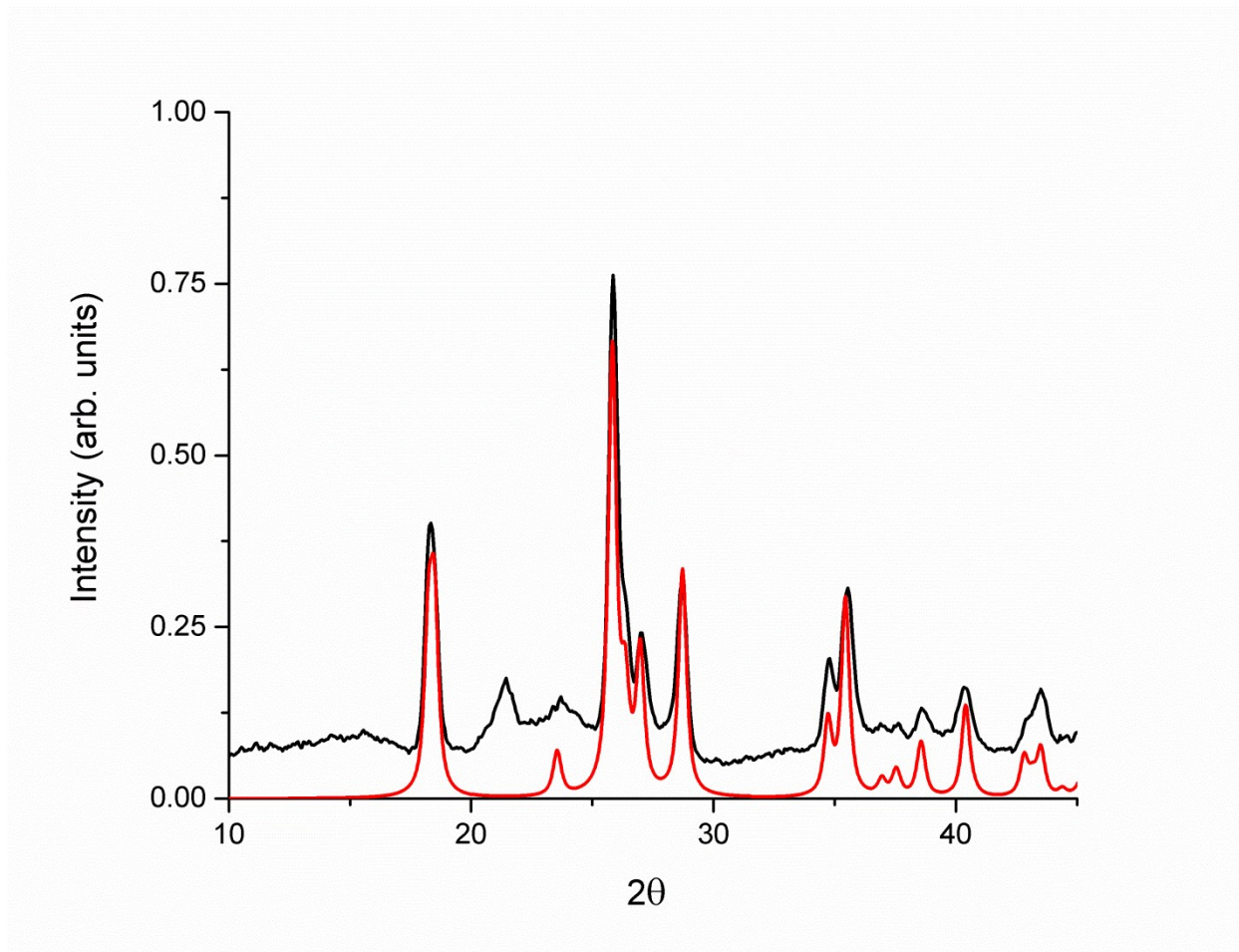


Figure S.5. Experimental (black) and calculated (red) PXR D of FeSO₄ · 4H₂O.

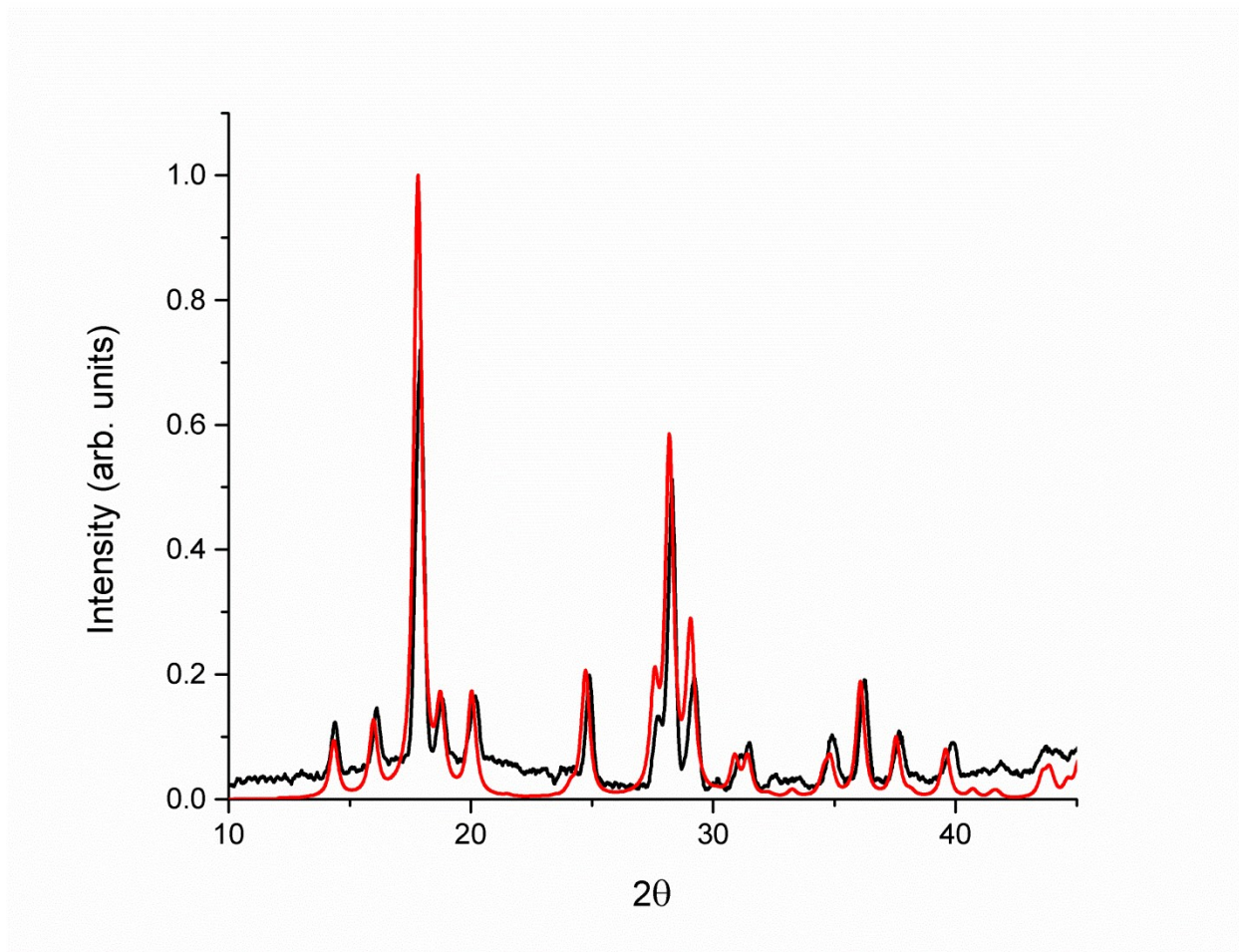


Figure S.6. Experimental (black) and calculated (red) PXRD of Fe₂(SO₄)₃OH · 2H₂O.

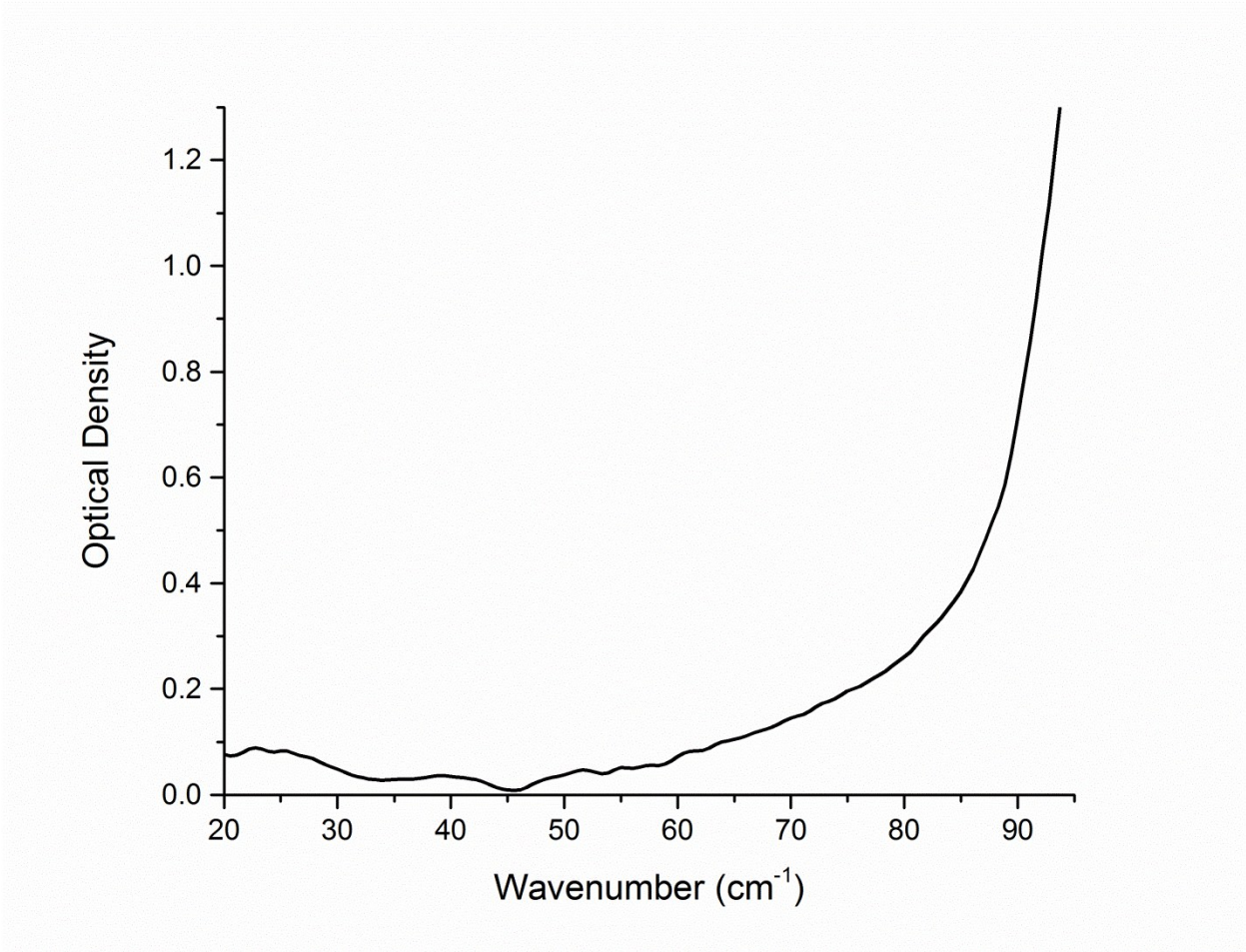


Figure S.7. Terahertz spectrum of FeSO₄ · H₂O taken at 77 K.

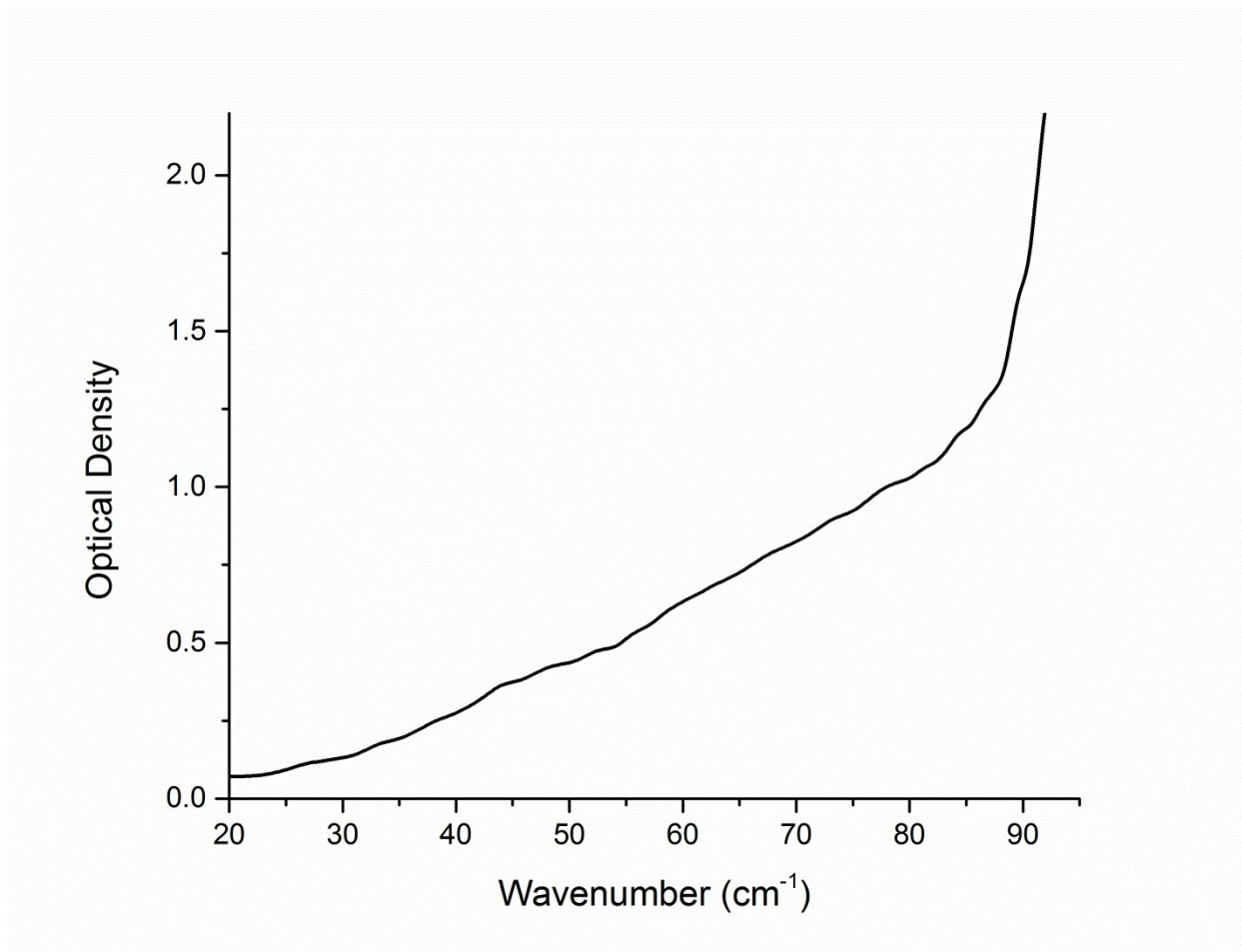


Figure S.8. Terahertz spectrum of $\text{Fe}_2(\text{SO}_4)_3\text{OH} \cdot 2\text{H}_2\text{O}$ at 77 K.

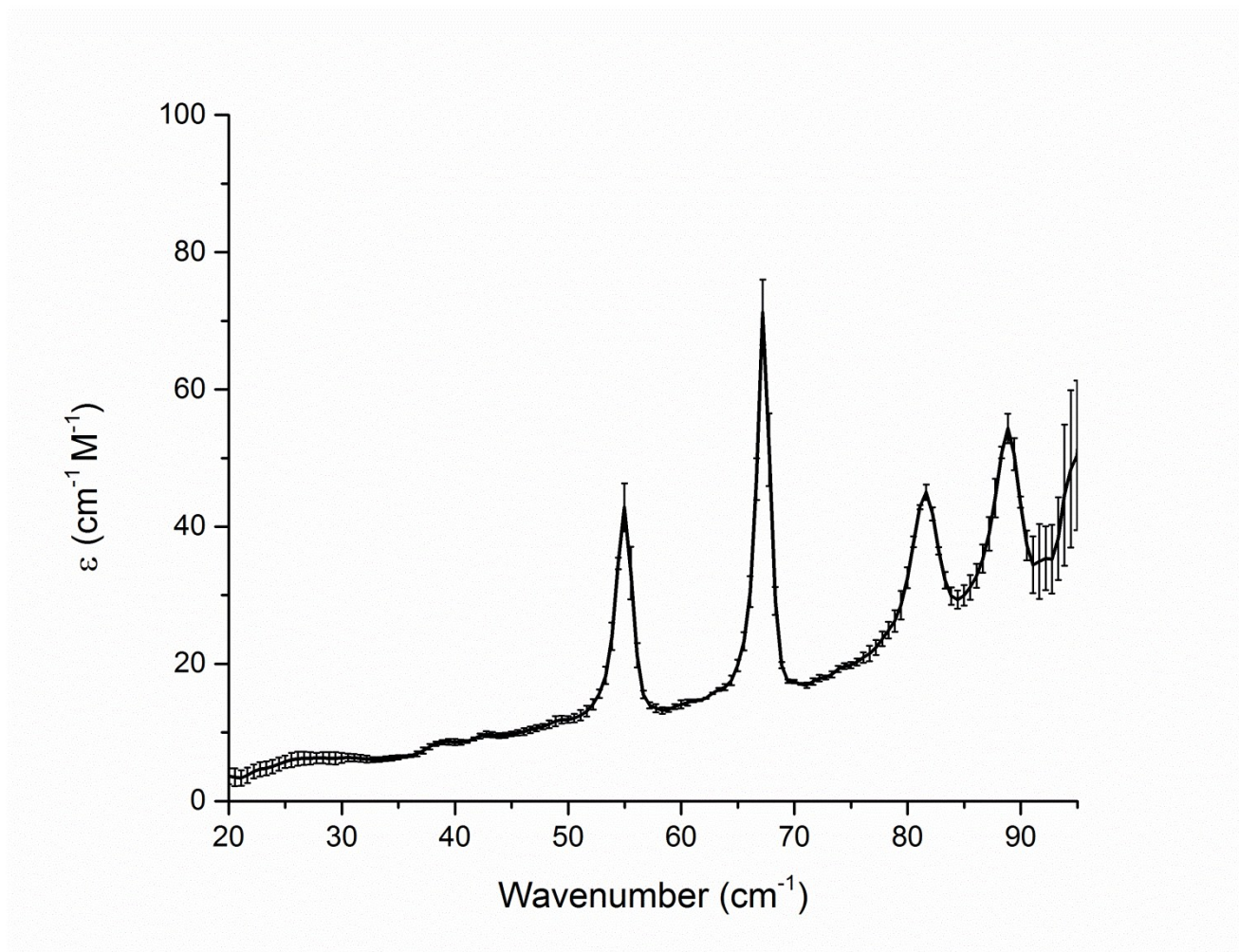


Figure S.9. 78 K terahertz spectrum of $\text{FeSO}_4 \cdot 4\text{H}_2\text{O}$ with standard deviation in the absorption shown.

Table S.1. Simulated IR-active vibrational frequencies (cm^{-1}) and intensities (km mol^{-1}) of anhydrous FeSO_4 .

Frequency	Intensity
136.89	0.06
150.15	108.13
157.41	41.93
191.81	146.45
209.69	413.13
227.76	0.08
245.50	177.13
305.82	239.99
343.84	205.31
471.56	85.16
472.56	0.00
584.42	83.47
587.20	149.13
663.45	252.24
942.36	268.15
978.20	2179.02
1095.32	1744.22
1142.05	1562.27

Table S.2. Simulated IR-active vibrational frequencies (cm^{-1}) and intensities (km mol^{-1}) of $\text{FeSO}_4 \cdot \text{H}_2\text{O}$.

Frequency	Intensity
121.63	7.14
127.52	40.94
165.68	130.80
178.83	40.36
191.74	24.47
229.45	226.35
235.39	176.87
277.29	615.90
303.30	52.85
306.78	125.88
325.34	27.15
329.17	90.45
426.25	0.09
527.57	47.17
586.41	300.91
608.21	112.09
613.05	691.31
708.16	231.31
886.72	1954.31
943.45	35.10
961.57	268.56
1042.18	598.61
1086.05	1564.54
1140.22	1759.60
1617.19	167.13
3428.36	1385.50
3449.11	3867.82

Table S.3. Simulated IR-active vibrational frequencies (cm^{-1}) and intensities (km mol^{-1}) of $\text{FeSO}_4 \cdot 4\text{H}_2\text{O}$.

Frequency	Intensity
58.27	8.75
63.54	2.36
68.62	0.00
72.25	11.94
81.75	0.00
85.87	2.96
96.44	4.16
98.26	0.00
101.95	0.00
103.36	24.39
108.00	0.00
115.00	27.16
119.47	4.55
120.56	0.00
123.95	0.00
129.67	0.10
131.77	162.59
132.07	0.20
135.90	48.91
139.19	0.00
147.83	0.01
148.56	94.71
148.72	40.45
153.24	18.68
153.73	0.33
156.94	22.73
158.05	0.01
158.64	0.01
160.54	154.88
164.09	0.00
164.85	0.02
172.12	200.30
173.02	0.01
174.70	3.62
177.39	0.01
184.95	2.17

185.55	39.80
189.46	244.79
189.50	0.01
190.78	0.23
193.94	100.20
195.22	43.78
196.41	0.02
201.05	250.94
206.06	0.00
208.54	0.02
216.17	0.01
218.10	68.23
219.91	0.81
225.32	0.00
228.24	0.01
228.74	5.57
230.60	67.03
236.90	0.00
238.23	0.01
247.24	376.19
247.36	111.03
249.00	0.00
250.15	0.07
250.46	3.54
255.04	27.13
260.36	47.34
261.31	0.01
267.79	137.70
270.35	0.01
310.22	0.23
311.47	85.87
313.29	3.61
314.57	23.30
358.53	192.21
364.82	0.01
369.39	0.04
370.34	0.02
374.04	69.38
377.05	2.41
377.89	141.38
378.69	0.05

407.80	39.68
412.78	46.22
413.06	1.59
417.90	0.02
442.82	80.24
443.42	19.32
443.56	192.75
445.71	0.04
459.59	0.00
462.81	35.24
463.08	542.67
472.00	15.61
476.51	0.00
478.12	244.04
478.59	0.15
497.09	0.01
516.63	0.03
522.85	7.37
524.98	767.98
528.23	19.76
556.30	0.16
567.73	666.68
569.73	1.77
571.63	971.77
585.43	84.33
586.41	0.22
588.80	0.01
590.39	213.03
590.99	45.16
591.48	362.87
592.91	0.01
594.80	0.23
596.33	1075.58
598.56	0.04
598.95	0.03
601.47	132.97
605.93	430.52
610.95	0.03
613.53	0.02
629.26	100.41
639.28	1947.07

648.56	0.01
649.95	175.51
659.46	0.10
677.16	0.00
688.79	0.39
697.07	159.71
712.53	0.01
714.89	140.08
716.47	474.71
718.04	49.79
728.06	0.20
742.49	116.20
748.12	0.01
757.09	191.48
765.37	81.73
769.95	0.29
783.31	44.52
789.89	449.15
792.07	0.92
794.98	0.39
802.97	86.60
805.27	2.95
812.47	47.66
821.32	0.07
822.92	0.08
831.79	4.45
842.55	270.18
871.90	0.00
880.77	97.08
890.40	0.03
893.57	48.76
949.03	11.97
950.05	0.14
950.53	85.36
951.22	0.00
1033.66	3578.84
1034.61	81.23
1046.34	0.00
1048.40	0.02
1073.95	0.00
1082.00	0.03

1085.56	865.60
1087.54	3199.14
1123.55	1827.06
1129.91	0.00
1138.02	25.98
1163.39	0.00
1618.29	0.01
1622.71	370.79
1623.85	3.03
1629.62	92.16
1645.85	415.58
1653.31	0.01
1656.64	50.83
1666.72	0.33
1667.42	181.88
1671.43	12.64
1676.89	278.12
1678.56	0.02
1681.08	0.00
1684.82	538.74
1749.67	0.00
1749.89	0.00
3451.20	4285.27
3452.21	11.22
3459.34	2445.12
3467.56	0.05
3533.42	472.93
3535.08	60.81
3535.19	452.70
3536.23	280.11
3549.86	719.34
3554.76	3537.25
3556.28	10.23
3559.88	61.73
3614.00	0.30
3614.18	0.00
3619.50	386.88
3623.02	2915.85
3623.71	0.00
3623.98	6.44
3639.95	1595.83

3641.58	0.06
3642.35	876.95
3646.76	12.04
3655.39	541.48
3659.75	6647.16
3706.42	0.50
3709.33	1024.14
3714.87	2606.74
3729.42	0.96
3787.12	1576.44
3791.10	516.00
3796.34	0.26
3807.43	0.03

Table S.4. Simulated IR-active vibrational frequencies (cm^{-1}) and intensities (km mol^{-1}) of $\text{FeSO}_4 \cdot 7\text{H}_2\text{O}$.

Frequency	Intensity
51.63	2.60
54.01	1.91
58.09	0.00
62.97	12.01
70.42	9.05
77.69	0.29
87.05	5.38
90.99	3.67
94.23	6.70
103.00	0.06
109.62	35.94
117.65	1.80
118.49	3.23
125.94	77.26
128.72	20.09
131.48	43.09
135.02	143.00
140.27	94.72
142.37	140.68
149.56	12.14
149.57	57.79
155.37	73.05
157.17	1.15
163.32	1.73
163.72	51.46
163.93	85.14
173.06	9.38
174.45	39.05
177.59	0.86
185.89	52.44
187.18	96.88
190.82	3.16
192.47	5.05
202.64	11.64

204.30	137.31
205.90	2.30
206.95	56.83
221.09	31.12
222.45	315.06
235.00	221.42
238.31	45.98
239.85	78.91
246.75	65.47
250.43	79.54
262.45	33.93
279.89	120.71
284.71	21.69
286.29	74.52
290.52	147.35
298.66	83.47
301.37	0.09
307.41	21.81
317.90	59.65
351.89	23.85
356.65	361.90
384.57	39.05
389.65	122.21
403.25	11.66
405.51	120.80
417.25	146.14
423.99	168.07
434.84	7.23
437.43	74.16
453.63	38.49
456.67	21.44
461.98	116.88
463.30	6.78
477.16	783.35
483.65	74.48
488.61	257.46
504.28	167.44
557.75	499.76
565.85	26.57
570.34	1098.79
573.70	42.10

577.70	117.63
585.06	104.38
594.71	218.94
599.18	393.71
599.24	595.47
602.77	703.03
607.10	64.62
614.63	766.13
629.19	145.38
642.01	501.69
654.19	594.41
675.60	85.43
676.96	279.35
692.66	196.83
700.06	34.49
717.91	545.30
723.31	91.51
728.64	155.93
737.81	375.96
751.26	587.76
761.66	224.89
762.50	1173.24
768.99	578.21
776.59	239.45
783.91	88.77
790.56	103.20
808.21	807.26
819.11	208.71
842.04	36.72
844.01	37.67
853.56	346.83
864.26	49.37
885.62	226.40
891.01	235.66
896.29	5.32
910.77	187.14
935.94	28.88
938.30	223.05
954.82	877.21
966.33	722.25
1029.70	2865.38

1032.94	20.97
1053.21	192.58
1069.10	1343.64
1071.91	1346.03
1079.19	1.31
1116.24	1482.03
1123.68	940.77
1602.89	53.07
1604.50	311.04
1657.53	72.43
1660.32	482.53
1678.17	265.68
1680.85	16.67
1694.46	67.09
1694.47	55.63
1701.06	23.90
1705.03	223.49
1705.05	100.49
1707.90	167.71
1735.99	289.78
1737.16	97.56
3304.97	5063.57
3319.87	2273.69
3400.38	114.00
3414.15	6948.60
3461.74	931.49
3463.44	10.13
3477.20	5618.75
3480.08	355.64
3514.32	4109.33
3518.63	4162.44
3537.70	6155.89
3543.87	528.38
3548.73	2073.99
3561.39	23.70
3591.22	2400.28
3591.75	1103.93
3594.35	292.36
3594.52	47.16
3609.49	7691.99
3612.09	106.18

3615.76	3215.99
3622.41	323.70
3666.19	503.79
3667.18	1119.07
3680.34	1279.37
3681.46	2585.53
3712.15	2875.65
3714.40	649.02

Table S.5. Simulated IR-active vibrational frequencies (cm^{-1}) and intensities (km mol^{-1}) of $\text{Fe}_2(\text{SO}_4)_3\text{OH} \cdot 2\text{H}_2\text{O}$.

Frequency	Intensity
109.33	16.97
127.94	0.31
138.42	60.39
159.18	110.57
164.11	104.01
174.80	128.52
180.97	82.28
209.85	224.33
244.69	169.78
250.86	12.10
271.10	91.62
294.69	190.06
302.67	269.31
327.93	293.12
433.73	73.11
436.00	16.00
445.62	218.70
471.61	906.30
476.27	209.25
484.40	0.26
524.67	877.07
537.29	527.26
580.01	270.89

590.22	228.46
651.00	0.58
705.51	32.25
723.42	168.13
794.30	833.24
835.60	47.66
909.68	106.28
925.47	2398.45
963.04	268.88
1033.67	334.01
1058.23	2600.35
1128.62	1453.04
1672.50	22.54
1713.74	383.75
3400.72	1816.96
3447.43	3091.65
3453.35	5598.98
3538.55	4434.23
3802.21	342.48

Table S.6. Solid-state DFT optimized atomic positions of anhydrous FeSO₄, which crystallizes *Cmcm*, with lattice parameters $a = 5.251 \text{ \AA}$, $b = 8.020 \text{ \AA}$, $c = 6.642 \text{ \AA}$.

	a	b	c
Fe	0.000	0.000	0.000
Fe	0.000	0.000	-0.500
S	0.000	0.350	0.250
O	0.000	0.250	0.064
O	0.000	-0.250	-0.436
O	-0.265	-0.040	0.250

Table S.7. Solid-state DFT optimized atomic positions of $\text{Fe}_2(\text{SO}_4)_3\text{OH} \cdot 2\text{H}_2\text{O}$, which crystallizes $P2_1/m$, with lattice parameters $a = 6.826 \text{ \AA}$, $b = 7.404 \text{ \AA}$, $c = 5.809 \text{ \AA}$, $\beta = 90.254^\circ$.

	a	b	c
Fe	0.000	0.000	0.000
O	0.180	0.085	0.251
O	0.230	-0.026	-0.222
H	-0.345	0.403	0.174
H	-0.278	-0.421	0.309
S	0.305	0.250	0.285
O	0.378	0.250	-0.475
O	0.468	0.250	0.117
O	0.049	-0.250	0.115
H	0.136	-0.250	0.247